



Audio Engineering Society

Convention Express Paper 14

Presented at the 153rd Convention
2022 October

This Express Paper was selected on the basis of a submitted synopsis that has been peer reviewed by at least two qualified anonymous reviewers. The complete manuscript was not peer reviewed. This express paper has been reproduced from the author's advance manuscript without editing, corrections, or consideration by the Review Board. The AES takes no responsibility for the contents. This paper is available in the AES E-Library (<http://www.aes.org/e-lib>), all rights reserved. Reproduction of this paper, or any portion thereof, is not permitted without direct permission from the Journal of the Audio Engineering Society.

Wave-shaping using novel single-parameter waveguides

Mark Dodd^{1,2} and Jack Oclew-Brown²

¹Celestion International, Ipswich, IP6 0NL, UK

²GP Acoustics (UK) Ltd, Maidstone, ME15 6QP, UK

Correspondence should be addressed to Mark Dodd (mark.dodd@celestion.com)

ABSTRACT

PA systems looking to cover a wide audience area with coherent sound are limited by current horn technology. With conventional single-surface horns, one can achieve either high input impedance or wide directivity but not both. Existing wave-shaping devices try to overcome these issues, but most are unable to transmit a wave coherently (without reflection, diffraction or resonance).

In this paper, we present a new type of wave-shaping waveguide based on maintaining single-parameter wave behaviour throughout the waveguide over a wide frequency range. Various examples are included illustrating the performance benefits of this type of waveguide compared to conventional solutions.

0 Introduction

Acoustical horns provide two essential ingredients of PA loudspeaker systems: high efficiency and directivity control. As a consequence the vast majority of PA systems use horns or waveguides of one form or another. Nevertheless horns do have significant limitations. Kolbrek demonstrates in [1] that so-called "single-surface" horns are fundamentally limited and a wide bandwidth ratio horn must necessarily have narrow directivity. There have been many attempts to work around this problem, for example by using multicell designs, or diffraction slots. More recently, wave-shapers, intended to produce a rectangular planar wavefront, provide a source for a vertical array of cylindrical waveguides [2]. These approaches introduce new compromises that must be balanced against directivity and bandwidth, especially of acoustical resonance, response irregularity and incoherence.

In this paper we outline a novel approach that allows new possibilities in horn design, allowing wide bandwidth ratio and wide directivity simultaneously.

The first section of this paper is an introduction to single-parameter (1P) waves. This starting point is essential because if we wish to design a horn providing near constant directivity over a wide bandwidth it is logical that the supported waves within the horn will be close to 1P. A few examples of 1P waveguides are provided.

Secondly we review some simple single-walled horns and discuss them in comparison with the 1P examples in section 2.

Finally we outline the new approach in section 3.

1 Single parameter (1P) waves

Single parameter waves (1P) waves have the property that all spatial variation is described by only one spatial coordinate. This spatial coordinate defines the distance that the wave has travelled, and is sufficient to characterise the wave completely.

1P waves have unique properties that cannot be assumed more generally of any other type of wave. 1P waves are homogenous in the sense that there is no

pressure gradient perpendicular to the direction of propagation. This property means that at any instant, on any surface perpendicular to the spatial coordinate, the acoustical pressure is perfectly uniform. These surfaces can be thought of as wavefront surfaces. Since there is no spatial variation in pressure except for along the direction of the spatial coordinate, this determines that energy cannot be moved across the wavefront surfaces, and as a consequence any change in pressure amplitude as the wave propagates is completely determined by the mean curvature of the wavefronts (See AI), and this must necessarily also be uniform over every wavefront surface. The consequence is that all wavefront surfaces have the same shape. The speed at which the wave propagates along the coordinate is constant, and therefore any two wavefronts must be the same distance apart over the entire surface.

The behaviour is totally independent of the signal carried by the wave, and the behaviour is identical irrespective of frequency.

In free-space, there are only three types of single parameter waves that can possibly occur in nature [3]. These are plane waves, cylindrical waves and spherical waves.

1.1 1P waves in enclosed spaces

The three types of single parameter wave will readily propagate in an enclosed space, while retaining all of the properties listed above, provided that some conditions are met. The boundaries of the enclosure must be a combination of surfaces that are perfectly perpendicular to the wavefront surfaces and surfaces that are coincident with wavefront surfaces. The perpendicular surfaces must be rigid. The coincident surfaces may be rigid, or have a uniform finite impedance, or a uniform uniform prescribed normal velocity, or a uniform prescribed surface pressure.

Figure 1 shows an example of a cylindrical wave propagating within an enclosed space. Note that both the iso-phase surfaces and pressure amplitude contours are perfectly cylindrical. This behaviour is invariant of frequency.

In figure 2, the cylindrical source is replaced with a planar source resulting in beaming. In figure 3, the geometry is truncated into an infinite 2π baffle resulting in mouth reflections. In both cases the 1P behaviour breaks down.

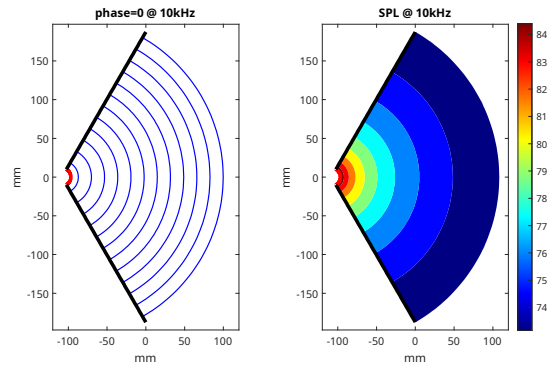


Figure 1. 3D FEM simulated phase and SPL contours at 10kHz generated by cylindrical section (red) moving radially with 1mm/s harmonic normal velocity bounded by two infinite rigid planes (black). Source width is 20mm

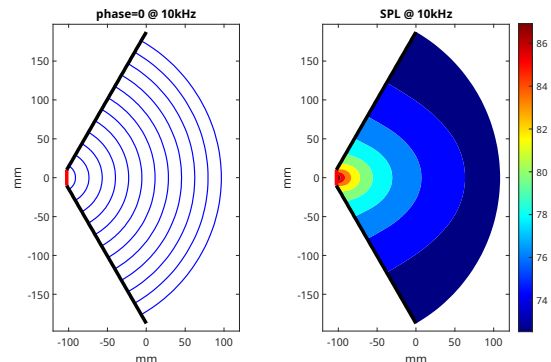


Figure 2. 3D FEM simulated phase and SPL contours at 10kHz generated by planar section (red) moving horizontally with 1mm/s harmonic normal velocity bounded by two infinite rigid planes (black). Source width is 20mm

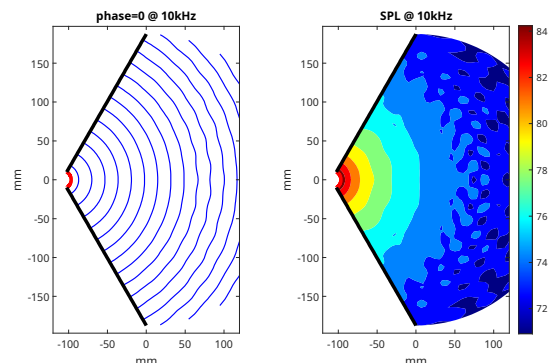


Figure 3. 3D FEM simulated phase and SPL contours at 10kHz generated by truncating the geometry from figure 1 into an infinite 2π baffle at $x=0$.

1.2 Acoustic impedance of 1P waveguides

The radiation efficiency of a horn is determined by the real part of the throat impedance. An ideal horn for use in a PA loudspeaker would have a throat impedance with a high resistance over a very wide bandwidth. This relationship between impedance and efficiency is extremely well understood [4, p. 468].

Determining throat impedance is a critical consideration in horn design. Webster [5] was the first to provide a means of throat impedance calculation when he simplified the wave equation of a horn from three dimensions into one. In doing so he linked the propagation of the wave down the length of the horn to the cross-sectional geometry of the horn as

$$\frac{\partial^2 p}{\partial u^2} + m(u) \frac{\partial p}{\partial u} + \frac{\partial p}{\partial t} = 0 \quad 1.1.$$

where u is a spatial coordinate along the length of the horn, p is the acoustic pressure, and $m(u)$ is the flare-rate of the horn defined as

$$m(u) = \frac{1}{S(u)} \frac{\partial S(u)}{\partial u} = \frac{\partial \ln S(u)}{\partial u} \quad 1.2.$$

where $S(u)$ describes how the horn area changes along its length.

Many authors have applied Webster's horn equation to different geometries in order to calculate throat impedance, each choosing different assumptions about the geometric parametrisation. Kolbrek gives a thorough explanation of this approach [4, p. 747]. However, such analysis is severely limited because an implicit assumption in Webster's derivation is that the wave in the horn is 1P and, as emphatically demonstrated by Putland [3], Webster's equation is exact when applied to any 1P wave and always approximate when applied elsewhere.

Figure 4 shows the FEA computed normalised throat impedance of the 1P waveguide in figure 1. Note that the real part of the impedance is significantly less than unity over most of the bandwidth.

For a horn to provide normalised throat resistance close to unity, it is necessary for the flare rate throughout to be less than twice the wavenumber to be carried [4, p. 474],

$$m(u) \leq 2k. \quad 1.3.$$

Expressed in other terms, the horn should double in area over a distance greater than 0.055 wavelengths.

With the three types of 1P wave there is no flexibility over $m(u)$, it is strictly linked to the geometry of the wavefront. The flare-rate of horns carrying a plane, cylindrical and spherical wave is

$$m=0, m(r)=\frac{2}{r} \text{ and } m(r)=\frac{1}{r} \quad 1.4.$$

respectively, where r is the radial distance from the horn coordinate system origin. The plane-wave-carrying horn provides ideal loading, but can be ruled out immediately for PA applications as the wavefront has no divergence. The cylindrical and spherical wave horns suffer from another problem – the flare rate at the throat of the horn is too high. Appreciable acoustic loading is only provided when

$$r_0 > \frac{\lambda}{2\pi} \text{ and } r_0 > \sqrt{\frac{\lambda}{4\pi}} \quad 1.5.$$

respectively, where λ is the acoustic wavelength and r_0 is the radial coordinate at the horn throat. Achieving sufficiently high values of r_0 to gain appreciable throat impedance over a useful bandwidth, requires either a narrow angle between the planar or conical waveguide walls, or an extremely large horn throat size.

As a result we conclude that, although 1P waveguides carry waves with attractive properties – frequency independence, perfect homogeneity, zero diffraction and reflection – they are not ideal for use in PA applications because they don't provide a wide bandwidth ratio.

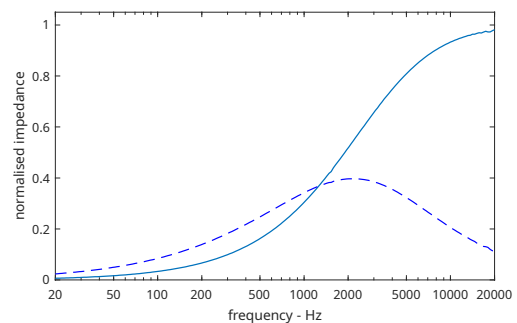


Figure 4. Normalised throat impedance corresponding to the extruded cylindrical waveguide shown in figure 1. Real part solid line, imaginary part dashed.

2 Analysis of wavefront behaviour in non-1P horns

The orthogonal trajectories of 1P wavefronts are straight lines [3, p. 441]. Horns that carry 1P waves, therefore, must have walls that are not curved along the direction of wave propagation. This leads to poor acoustical loading, as discussed above, and the source curvature must match the horn coverage, as demonstrated in figures 1 and 2.

It would be more useful to have a horn that receives a small shallow-angle acoustical wave at the throat and transmits a large wide-angle acoustical wave at the mouth. This requires a horn with a wall that curves and whose included angle increases along the horn length. Horns of this type are widely used in PA systems. Such horns don't carry 1P waves, but they do have other useful characteristics.

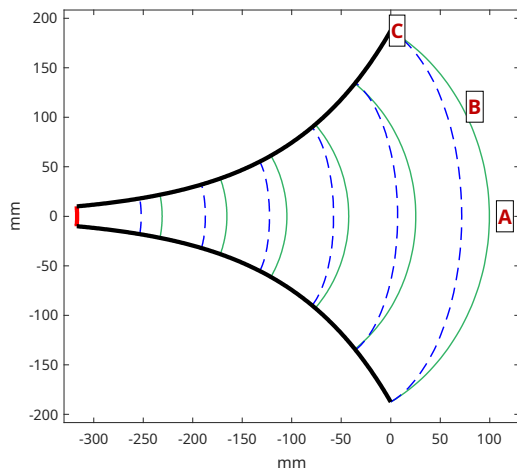


Figure 5. Thin extruded exponential horn with 500Hz cut-on frequency formed by two extruded side walls (black), a 20mm width planar source (red), terminated into a 60deg semi-infinite conical-wave guide. Contours of constant phase are shown for 50Hz (green, solid) and 20kHz (blue dash).

Figure 5 shows iso-phase surfaces at 50Hz and 20kHz in an extruded exponential horn computed using 3D FEM with PAFEC-FE [6]. At 50Hz (green lines) the wave behaviour is close to ideal – shallow-angle waves at the throat slowly expand to large-angle waves at the mouth. The wave is always perpendicular to the rigid walls and, because the wavelength is large, this boundary condition effects the wave across the entire horn width. At every surface plotted, the wave is almost perfectly cylindrical.

The 20kHz iso-phase surfaces (blue dash) have a different characteristic. The wave still obeys the same boundary condition, and remains perpendicular to the walls, but the central region of the wave propagates almost as if it is in free space. The wavefront is flatter and the distance between consecutive waves is more constant. The behaviour is not 1P as:

- the wave shape varies at different frequencies,
- the wave curvature is not constant over the wave-front,
- there is no single spatial parameter that could describe the behaviour.

The higher curvature of the 20kHz wave near the walls means that, as the wave propagates, the pressure level falls faster than at the central region. This has an important effect on the directivity of the horn. Figure 6 shows the frequency response at three positions at the horn mouth. Above the cut-on frequency of the horn (500Hz) the response curves progressively separate indicating severe 'beaming'.

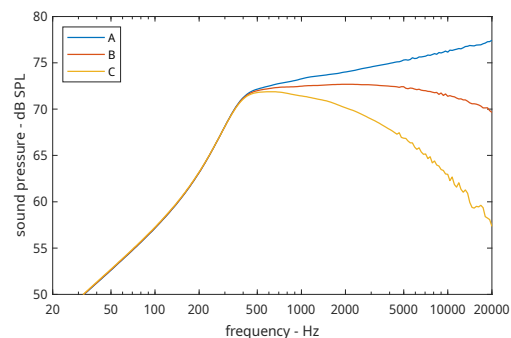


Figure 6. Sound pressure level responses at 0deg, 30deg and 60deg at the mouth of the extruded exponential waveguide shown in figure 5.

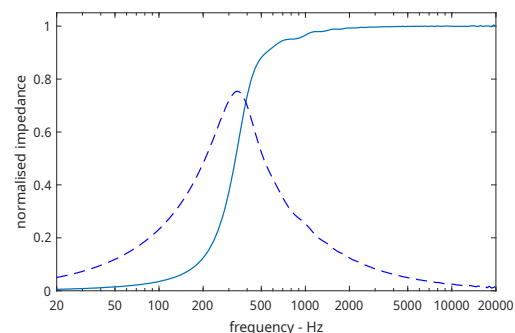


Figure 7. Normalised throat impedance corresponding to the extruded exponential waveguide shown in figure 5. Real part solid line, imaginary part dashed.

However, in terms of throat impedance, this horn has a big advantage compared to a 1P horn. The flare-rate is much slower near the throat. The normalised acoustical impedance, shown in figure 7, has a resistance close to unity from 500Hz upwards. Compared to figure 4, for the cylindrical waveguide, this horn provides an extended range of high impedance.

3 A new approach to correcting a thin waveguide

In this section a new approach is described that allows approximately 1P waves to propagate in waveguides with walls that are curved along the direction of wave propagation. This new approach is applicable to thin waveguides with two primary walls spaced less than a wavelength apart and two secondary walls that may be curved and spaced many wavelengths apart.

The method begins with a prototype waveguide, constructed according to the limitations above, with appropriate throat and mouth shape and orientation, according to the application, and with primary and secondary walls that are smooth and perpendicular to each other.

At equally spaced intervals between the prototype waveguide throat and mouth, “notional 1P wavefronts” (N1P wavefronts) are constructed by deduction or calculation. These N1P wavefronts must follow strict rules according to our knowledge of 1P waves: they must be perpendicular to the walls and they must have constant mean-curvature. In most cases the N1P wavefronts are sections of known 1P waves (planar, spherical or cylindrical).

The next step is to assume a propagation trajectory that the wave will follow between the N1P wavefronts and plot these trajectories on a design surface, midway between the primary surfaces. The trajectories must be smooth and perpendicular to the N1P wavefronts. At the edges of the waveguide the trajectories will lie on the secondary walls.

The length of the each trajectory between each pair of N1P wavefronts is calculated. For 1P propagation, all trajectories between two N1P wavefronts must have the same length. In the prototype waveguide this will not be the case. To correct the waveguide, the design surface is deformed in the normal direction to equalise the trajectory lengths. This provides a trajectory length that is constant between N1P wavefronts and results in

corrugations, aligned to the N1P wavefronts, and a deformation which is tallest where the N1P wavefronts are closely spaced. The primary and secondary surfaces are re-created by thickening the design surface.

After correction, the trajectory length is constant between N1P wavefronts over their entire surface, and the N1P wavefronts satisfy the conditions for 1P propagation and approximately 1P behaviour is observed up to an upper frequency limit determined by the first transverse modes between primary walls.

3.1 Example 1, curved duct

The new method is most easily understood with a simple example. Figure 8 shows a suitable prototype waveguide which has a rectangular throat (red), rectangular mouth (green) and turns a 90deg bend. The primary walls are planar and the secondary walls are cylindrical. The primary walls are parallel, spaced 2mm apart, are perpendicular to the secondary walls, and both pairs of walls are perpendicular to the mouth and throat.

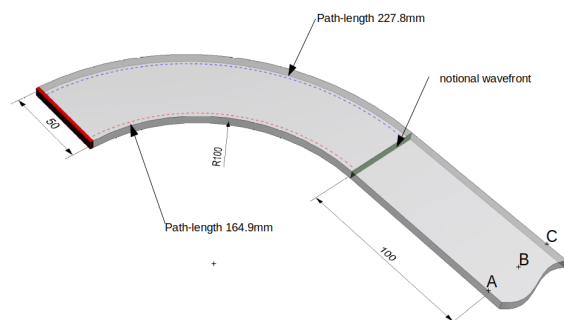


Figure 8. Prototype 2mm thick waveguide, with 90deg corner, leading to semi-infinite straight duct. For clarity, duct illustrated as 5mm thick.

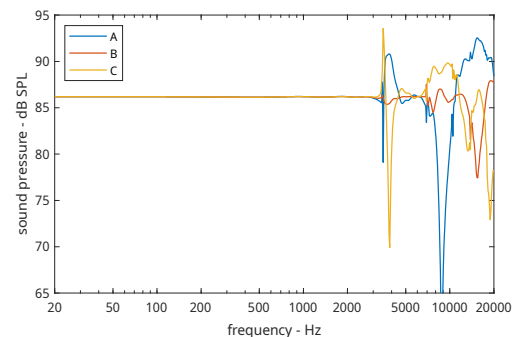


Figure 9. Sound pressure level response sampled at three points in the straight terminating section of the prototype waveguide shown in figure 8.

Figure 9 shows the response at three locations across the width of the prototype waveguide straight terminating section when a plane wave source is placed at the throat. Below 3kHz the pressure is identical at all three points, indicating 1P wave behaviour. Above 3kHz there are very large differences between the three curves and 1P behaviour is not occurring.

The steps of the new method are illustrated in figure 10 with each successive step shown between the five N1P planar wavefronts progressing in a clockwise direction. The design surface may be thought of as a 2D waveguide where the intersection of the notional 3D wavefronts forms a linear 2D wavefront.

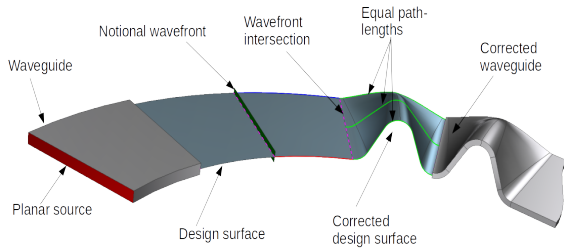


Figure 10. Successive design steps, shown between 5 notional wavefronts, progressing in a clockwise direction.

The sound pressure responses from the corrected waveguide at the same three locations shown previously for the prototype waveguide (figure 9) are shown in figure 11. It is clear from the reduction in the spread of the three responses that the wave emitted by the corrected waveguide is much more homogenous and close to 1P.

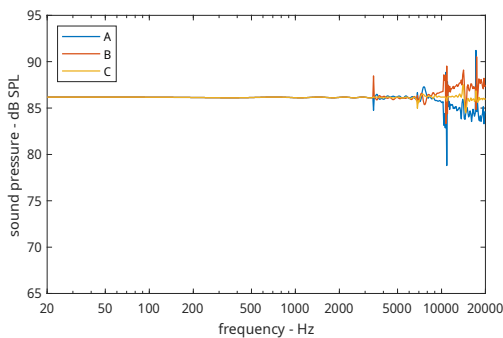


Figure 11. Sound pressure level response at points A, B and C of corrected corner duct using 10 corrugations.

3.2 Example 2, exponential horn

The method may also be applied to the exponential horn that was described in section 2. In this case the

curvature of the secondary walls results in a cylindrical 1P wavefront. The corrected geometry is shown in figure 12 and the sound pressure level responses plotted in figure 13 at the same locations across the mouth that were previously shown for the uncorrected design (figure 6). The three response curves now virtually overlap and this indicates that, at least within the plot bandwidth, the wave is behaving as if it were 1P and the N1P wavefronts have become the true wavefronts.

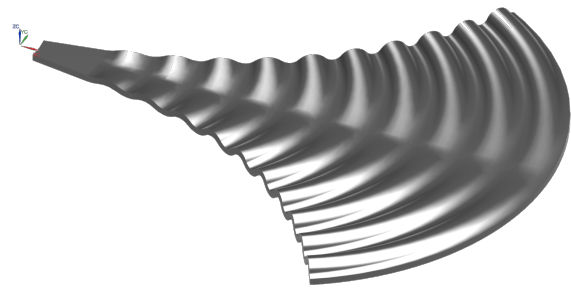


Figure 12. Corrected exponential horn using corrugated geometry

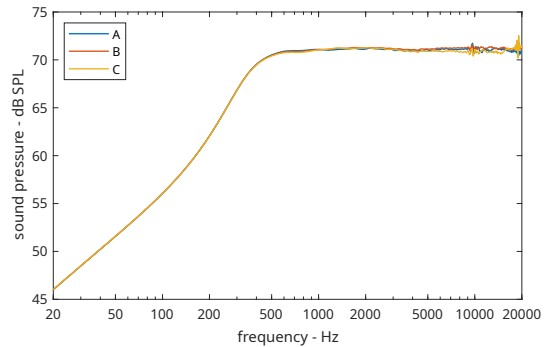


Figure 13. Sound pressure level responses at 0deg, 30deg and 60deg at the mouth of the corrected extruded exponential waveguide shown in figure 12.

Figure 14 shows the normalised acoustical impedance after the correction is applied. The horn area expansion function, $S(u)$, was not changed by the correction process and consequently the excellent acoustic loading properties of the original exponential horn are retained. The additional ripple when compared to figure 7 is due to increased reflection at the transition between the exponential waveguide and the infinite cylindrical termination.

The corrected waveguide has the acoustic impedance of an exponential horn, and corresponding loading benefits, while providing the dispersion of a cylindrical waveguide.

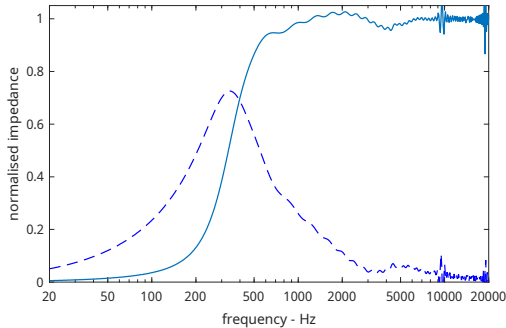


Figure 14. Normalised throat impedance corresponding to the corrected exponential waveguide shown in figure 12. Real part solid line, imaginary part dashed.

3.3 Example 3, aperture and wave-shape adapting waveguide

Several manufacturers have developed acoustical devices that receive a plane wave into an annular throat aperture and emit a plane wave at a rectangular mouth aperture. These devices are mostly for use at high-frequencies in line array systems, and work with varying degrees of success.

In this section we shall consider a similar device that changes from an annular throat to a rectangular mouth *and* also converts from a plane wave to a cylindrical wave. Figure 15 shows the prototype waveguide with leading dimensions. Figure 16 shows the pressure response of the prototype waveguide at three equispaced points ‘A’, ‘B’, and ‘C’ at the waveguide mouth. The response curves diverge above 2kHz, and from 4 kHz upwards the pressure at the outer edge of the waveguide is 12dB lower than at the centre. It is clear that a 1P wave is not being transmitted. The relatively smooth response is due to the modes being well damped by radiation, a characteristic that was already seen in the conventional exponential horn (figure 6).

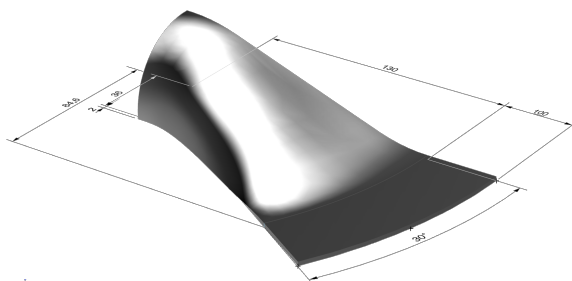


Figure 15. Prototype aperture and wave-shape adapting waveguide and conical waveguide termination.

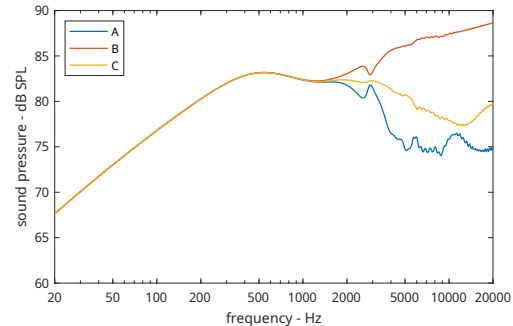


Figure 16. Sound pressure level responses at points A, B and C for the prototype aperture and wave-shape adapting waveguide shown in figure 15

The correction method is now applied and in this case the N1P wavefronts have 3D geometry and are not obvious to deduce. To sidestep this issue, iso-phase surfaces were calculated at 100Hz in the prototype waveguide. This frequency is low enough that wavelength is much greater than the adaptor dimensions and wavefront curvature is determined by the boundary conditions. Consequently the iso-phase surfaces are suitable for use as N1P wavefronts. The corrected geometry is illustrated in figure 17.



Figure 17. Corrected aperture and wave-shape adapting horn omitting conical termination.

The corresponding sound pressure level responses, plotted for the same positions as in the uncorrected design (figure 16), are shown in figure 18. Below 8kHz the responses overlay, while above this frequency the mean response separation is approximately 3dB up to 20kHz. This indicates that, at least within the plot bandwidth, the wave is behaving approximately as if it were 1P.

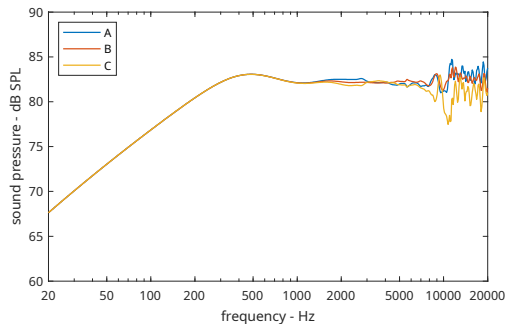


Figure 18. Sound pressure level responses in the corrected aperture and wave-shape adapting waveguide at the same positions as plotted for the prototype waveguide in figure 16.

4 Discussion

Three examples of possible applications have been used to illustrate the horn correction method, firstly a non flaring planar thin duct, secondly a planar horn, and thirdly 3D curved surfaces. Other possibilities are given in [7] and it seems likely other useful applications will be found in due course.

The alteration of wavefront shape or aperture occurs progressively throughout the corrected horn and because of the horn walls. While the behaviour may seem similar to that of a lens, it is quite different, as in a lens the wave is bent due to the change of wave speed at an interface.

In practice the path-length corrections may result in undesirable local changes of wavefront area. For example, the peak of a corrugation is inclined so the wavefront area will be slightly increased. Similarly, errors in path-length may be produced by the path of the wave ‘cutting the corner’ making the actual path-length smaller than the assumed path. It is also evident that sharply curved horn walls result in tall corrugations with excessive geometric distortion.

Using a thinner waveguide with more corrugations reduces these geometric errors, however, other improvements require an understanding of the location and magnitude of errors throughout the waveguide. One way to do this is to consider the local flare and path-lengths throughout the waveguide.

Once a horn has been corrected it behaves as a 1P waveguide and 1D design processes may be applied to refine the global flare rate. This may be achieved by adjusting the thickness and thus vary the global flare.

The manual design process used for these examples is time-consuming and intricate. A numerical design approach using calculated flare and path-length is being investigated to allow new designs to be explored in an expedient manner.

A non-homogeneous source will result in non-zeroth modes propagating along the waveguide with both the corresponding variations of pressure across the mouth and the additional group delay. In PA applications a coherent output is required and it is highly desirable to have a homogenous source.

Where a large wavefront is required, arrays of corrected horns may be used. In this instance the thickness and depth of corrugations becomes important and combining the output of individual waveguides must be done respecting both flare laws and path-length errors. Since the array elements are identical the risk of exciting circulating ‘phaseplug’ type modes is greatly reduced. A further advantage is the reduction in the number of individual paths and corresponding mechanical simplicity.

Having produced a large 1P wavefront the aperture diffraction must be considered. Keele showed how adding a section with higher global flare rate can greatly reduce midrange narrowing and the associated ‘lobing’ while retaining the wide dispersion at high frequencies [8].

5 Conclusion

By simply assuming 1P wavefront shape and then correcting the path-length between several notional 1P wavefronts a new type of waveguide has been created. The corrected horn waveguide has corrugations following the shape of 1P wavefronts with a height that results in equal path-lengths. This geometry result in the wavefront propagating so that it maintains constant curvature across each wavefront even at high frequencies, due to the equalised path-lengths. This allows the wave to be described simply in terms of distance propagated through the waveguide.

Further work will involve reducing the time to derive the corrected waveguide and improving it’s efficacy. The results may be further improved by geometry corrections to local flare and path-length throughout the waveguide. These tools may then be applied the produce corrected horns to allowing improved coherency and homogeneity of acoustic output to be produced in horn-loaded PA systems.

AI Flare-rate is wavefront curvature

Webster's horn equation is fundamentally based on the expression for the Laplacian operator given in his equation 19 [5]

$$\nabla^2 a = \frac{1}{S(u)} \frac{\partial}{\partial u} \left(S(u) \frac{\partial a}{\partial u} \right) \quad \text{I.1.}$$

Applying this expression directly on the coordinate u , the right-most differential term becomes unity and the result is the flare-rate of the horn

$$\nabla^2 u = \frac{1}{S(u)} \frac{\partial S(u)}{\partial u} = m(u) \quad \text{I.2.}$$

Dividing $\nabla^2 u$ by $|\nabla u|$ results in

$$\frac{\nabla^2 u}{|\nabla u|} = \nabla \cdot \frac{\nabla u}{|\nabla u|} = \nabla \cdot \mathbf{e}_u \quad \text{I.3.}$$

where \mathbf{e}_u is the unit vector pointing in positive u . This vector has another interpretation; it is the normal vector of surfaces of constant u . In other words, \mathbf{e}_u is the unit normal of the wavefront surfaces. The expression $\nabla \cdot \mathbf{e}_u$ also has another interpretation; it is equal to the negative total curvature (twice the mean curvature, H) of the wavefront surfaces [9],

$$\nabla \cdot \mathbf{e}_u = -2H(u) \quad \text{I.4.}$$

Putting equations I.2, I.3 and I.4 together demonstrates that flare-rate is a measure of wave-front curvature,

$$\frac{m(u)}{|\nabla u|} = -2H(u) \quad \text{I.5.}$$

If the coordinate u measures arc length (as is the case for the radial coordinate in a conventional spherical coordinate system, the radial or axial coordinate in a conventional cylindrical coordinate system, or any of the coordinates in a conventional Cartesian coordinate system) then $|\nabla u|$ is unity everywhere and

$$m(u) = -2H(u) \quad \text{I.6.}$$

6 References

- [1] B. Kolbrek, 'Limitations of Single-Surface Horns for Directivity Control', May 2020.
- [2] C. Heil, 'Sound wave guide', US5163167A, Nov. 10, 1992
- [3] G. R. Putland, 'Every One-Parameter Acoustic Field Obeys Webster's Horn Equation', *J. Audio Eng. Soc.*, vol. 41, no. 6, pp. 435–451, Jun. 1993.
- [4] B. Kolbrek, T. Dunker, and R. Kolbrek, *High Quality Horn Loudspeaker Systems 2019: History, Theory and Design*, First edition. Kolbrek Elektroakustikk, 2019.
- [5] A. G. Webster, 'Acoustical Impedance, and the Theory of Horns and of the Phonograph (reprint)', *J. Audio Eng. Soc.*, vol. 25, no. 1/2, pp. 24–28, Feb. 1977.
- [6] PACSYS Ltd., *PAFEC-FE*. PACSYS Ltd., 2008.
- [7] J. Oclec-Brown and M. Dodd, 'Acoustic waveguides', EP3806086A1, Apr. 14, 2021
- [8] D. B. K. Jr, 'Loudspeaker horn', US4308932A, Jan. 05, 1982
- [9] A. G. Megrabov, 'On divergence representations of the Gaussian and the mean curvature of surfaces and applications', *Bull. Novosib. Comput. Cent. Ser. Math. Model. Geophys.*, no. 17, pp. 35–45, 2014.